REFINEMENT OF THE STRUCTURE OF NACRITE BY HIGH-VOLTAGE ELECTRON DIFFRACTION

B. B. Zvyagin, S. V. Soboleva, and A. F. Fedotov

The structure of nacrite has been refined from three-dimensional data from high-voltage electron diffraction. Details of the actual structure have been elucidated that conform with details of the layer stacking and type of interatomic forces.

Nacrite is a polytype of the kaolin minerals and has repeatedly been the object of structure analysis. Although from the start it was clear that it consisted of $Al_2Si_2O_5(OH)_4$ two-level layers, the unusual nature of the structure long remained unrealized. Hendricks [1] made one of the first x-ray studies on the mineral, but this gave only a crude picture of the unit cell and the mutual disposition of the layers. Newnham [2] was the first to give a clear and reasonable ideal model based on general crystallochemical considerations, which was confirmed by experiment [3] after Zvyagin had distinguished all the polytype modifications of kaolin layers [4]. It was shown to be a unique polytype having diffraction features that correspond with the disposition and intensity of the reflections.

In 1969 there appeared an x-ray study on a single crystal, which led to further refinement of the structure [5].

The present study is concerned with refining the structure of nacrite. No matter how good the x-ray data of [5], this refinement is fully justified for the following reasons: 1) an independent method of structure analysis was used (electron diffraction), which provides a set of reflections differing in number and in the sets of indices; 2) the specimen was one found by Shcheglov [3], which was especially suitable for structure analysis and which gave texture patterns far superior to those recorded from many other specimens in this laboratory; 3) high-voltage electron diffraction was used for the first time to determine the structure. The accelerating voltage was 350 kV, which produced patterns of improved quality and which demonstrates the significance of higher accelerating voltages for structure analysis by electron diffraction.

The polytype theory considers all structures composed of kaolin layers in a single coordinate system having $b = a\sqrt{3}$, and it gives for nacrite a layer sequence expressed as $\sigma_1\tau_6\sigma_2\tau_3\sigma_1$ in terms of the symbols σ_i and τ_k for the intralayer and interlayer displacements of the two-dimensional grids of polyhedra [4, 6]. Nacrite has in this coordinate system a two-layer monoclinic cell having $\alpha > \pi/2$ and a c plane perpendicular to the short a axis. The names of the a and b axes are interchanged to obtain the standard setting, which produces a left-handed coordinate system with $\beta > \pi/2$. To obtain a right-handed system with $\beta > \pi/2$ one would have to reflect the structure at a plane perpendicular to the b axis or to take a $\sigma_5\tau_6\sigma_4\tau_3\sigma_5$ model with $\alpha < \pi/2$. However, there is no need to do this, because the atomic coordinates in the two enantiomorphic systems do not differ numerically.

The theoretical model was refined via texture-type electron-diffraction patterns. Elevated voltages give such patterns with numerous well-resolved reflections even with a maximum tilt of 73°. One quadrant of the pattern had 833 reflections with finite intensities, the maximum l being 20 and the maximum $h^2 + 3k^2$ being 172.
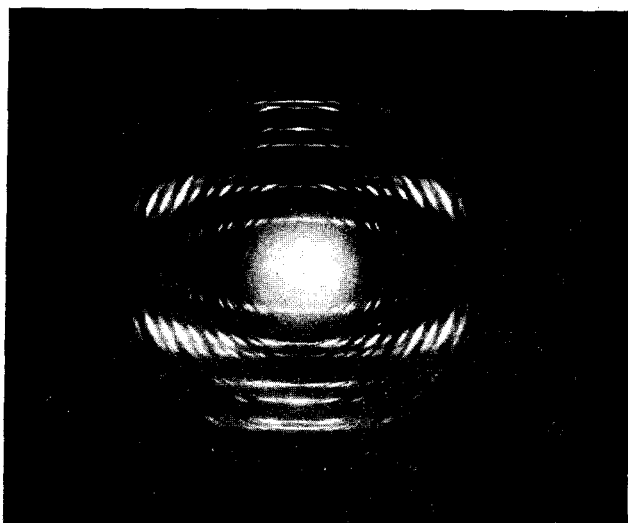
Fig. 1. Oblique-texture electron-diffraction pattern from nacrite
(φ = 73°).

The patterns (Fig. 1) reveal clearly how the actual lattice deviates from the ideal one: interchange of the a and b axes [3] and distortion of angle β. There are unusual differences between the reflections with h = 3n and h ≠ 3n, which not only indicate that c cos β ≠ − $a/3$ but also give the magnitude and direction of the deviation of β from the ideal value, with a, b, c cos β =−$a/3$ on account of the multiplicity of the components of the ideal σ and $\tau_{1/3}$. Failure to meet this condition is seen in the pat-terns as that p = q/3 is not obeyed, where p and q define the distance D of a reflection from the minor axis of the ellipse in the form D = hp + lq, since actually p = q/3 ± δ. As a consequence, the second ellipse has close triplets with distances ΔD = 3δ within the triplet, instead of the coincidence be-tween the reflections 02l, 3.1.l − 1, $\overline{3}$.1.l + 1 that would occur for δ = 0. The positions of these re-flections give p only as regards the sign in front of δ, which controls the signs of the h in the end re-flections in each triplet. The 11l reflection would coincide with $\overline{2}$.0.l + 1 on the first ellipse for δ = 0, as would $\overline{1}\overline{1}l$ with 2.0.l − 1, but these become twins with the internal interval ΔD = 3δ, while 20l reflections with l odd vanish, which indicates that there are c planes. In this case the exact positions of the reflections, which are characterized by D, are uniquely related not only to the magnitude of δ but also to the sign [7]. We found preliminary values of p from the first two ellipses, which were refined after the positions of the reflections had been measured on remote ellipses with large h. It was particularly significant that the 53l and $\overline{5}$.3.l +

3 reflections coincided on the seventh ellipse, and this implies that p/q = 0.300 ± 0.003 for nacrite.

As p and q are directly related to β and c, the texture-pattern geometry gave the cell param-eters as a = 8.90, b = 5.14, c = 14.59 Å, β =100°32'. The relation cos β/a =−0.300 leads to β being about 1° less than the ideal value.

The intensities were estimated from patterns with multiple exposures. The strongest and best resolved reflections on the first three ellipses were examined by microphotometer, and their in-tensities subsequently served as reference levels in estimating the intensities of other reflections. The lack of electron diffraction basal reflections was made good by calculating as in [8] from the in-tensities of basal x-ray reflections in powder pat-terns. To convert to the $|F^2|$ we used equations for the integrated intensities [9] that have been well tested by experiment. The intensities of over-lapping reflections (mainly on remote ellipses) were estimated by proportional assignment from the $|F^2|$ calculated first from the preliminary model and then from the refined one.

The initial model was constructed from two-level layers with ideal patterns for the bases of the octahedra (trigonal) and tetrahedra (hexagonal). The z coordinates were taken from the kaolinite structure [10]. The origin was displaced by y = 1/12 from the center of an empty octahedron. The tetrahedral grid in a two-level layer was placed above the octahedral one, while the c axis was set at the minimum obtuse angle β to the a axis. The real β was used in uniform shear of the model in the positive direction of the b axis.

The structure was refined from sections of the three-dimensional potential taken perpendicular to the b axis. After eight cycles, R was 16% and had almost ceased to change. The further refinement was by least squares in the isotropic approxima-tion, which reduced R to 12%.

Table 1 gives the atomic coordinates and tem-perature factors, while Table 2 gives the inter-atomic distances and Table 3 gives the base rota-tion angles of the tetrahedra and octahedra. The results are best discussed with detailed reference to the recent x-ray refinement of the nacrite struc-ture [5]. Unfortunately, the structure of [5] is de-scribed in a different coordinate system, with the origin at the center of a ditrigonal loop of tetra-hedron bases, the tetrahedral grid under the oc-tahedral one, and the c axis at β = 114° to the a axis. The last was [5] based on displacing the ori-gin selected by the authors by [−1/3, 0] in suc-

TABLE 1. Atomic Coordinates and Temperature Factors for Nacrite

Atom	Electron diffraction				Coordinates from [5]		
	B	x/a	y/b	z/c	x/a	y/b	z/c
Al_1	0.82	0.329	−0.082	0.003	0.328	−0.089	0.004
Al_2	0.81	0.164	0.421	0.004	0.170	0.425	0.004
Si_1	0.80	0.064	0.270	0.193	0.061	0.271	0.193
Si_2	0.75	0.234	−0.239	0.194	0.229	−0.236	0.193
O_1	0.61	0.146	0.009	0.227	0.135	0.000	0.224
O_2	0.64	0.173	0.503	0.239	0.181	0.494	0.235
O_3	0.72	0.415	−0.230	0.240	0.409	−0.207	0.235
O_4	0.62	0.026	0.304	0.078	0.025	0.314	0.081
O_5	0.66	0.208	−0.267	0.082	0.205	−0.266	0.082
OH_1	0.64	0.338	0.216	0.079	0.336	0.230	0.075
OH_2	0.64	0.169	0.095	−0.070	0.160	0.110	−0.064
OH_3	0.54	0.289	−0.330	−0.064	0.292	−0.379	−0.061
OH_4	0.64	0.474	0.057	−0.063	0.478	0.066	−0.060

TABLE 2. Interatomic Distances (Å) in Nacrite

Si_1 tetrahedron		Si_2 tetrahedron	
$Si_1 - O_1$	1.57	$Si_2 - O_1$	1.61
$Si_1 - O_2$	1.61	$Si_2 - O_2$	1.62
$Si_1 - O_3$	1.61	$Si_2 - O_3$	1.63
$Si_1 - O_4$	1.67	$Si_2 - O_5$	1.61
Mean	1.615	Mean	1.617
$O_1 - O_2$	2.62	$O_1 - O_2$	2.56
$O_1 - O_3$	2.50	$O_1 - O_3$	2.67
$O_2 - O_3$	2.60	$O_2 - O_3$	2.55
$O_1 - O_4$	2.70	$O_1 - O_5$	2.65
$O_2 - O_4$	2.68	$O_2 - O_5$	2.68
$O_3 - O_4$	2.74	$O_3 - O_5$	2.68
Mean	2.640	Mean	2.632
Al_1 octahedron		Al_2 octahedron	
$Al_1 - O_4$	1.98	$Al_2 - O_4$	1.87
$Al_1 - O_5$	1.96	$Al_2 - O_5$	1.97
$Al_1 - OH_1$	1.89	$Al_2 - OH_1$	2.01
$Al_1 - OH_2$	1.86	$Al_2 - OH_2$	1.99
$Al_1 - OH_3$	1.86	$Al_2 - OH_3$	1.88
$Al_1 - OH_4$	1.89	$Al_2 - OH_4$	1.92
Mean	1.906	Mean	1.940
$O_4 - O_5$	2.87	$O_4 - O_5$	2.73
$O_4 - OH_1$	2.71	$O_4 - OH_1$	2.80
$O_5 - OH_1$	2.75	$O_5 - OH_1$	2.90
$O_4 - OH_4$	2.41	$O_4 - OH_4$	2.41
$O_5 - OH_3$	2.46	$O_5 - OH_3$	2.46
$OH_1 - OH_2$	2.48	$OH_1 - OH_2$	2.48
$O_4 - OH_3$	2.85	$O_4 - OH_2$	2.85
$O_5 - OH_3$	2.86	$O_5 - OH_4$	2.95
$OH_1 - OH_4$	2.71	$OH_1 - OH_2$	2.82
$OH_2 - OH_3$	2.71	$OH_2 - OH_3$	2.89
$OH_2 - OH_4$	2.71	$OH_2 - OH_4$	2.83
$OH_3 - OH_4$	2.83	$OH_3 - OH_4$	2.88
Mean	2.700	Mean	2.750

Hydrogen bonds

$O_1 - OH_2$	2.99
$O_2 - OH_3$	2.92
$O_3 - OH_4$	2.95
Mean	2.953

cessive layers on normal projection onto the ab plane, but the displacements of corresponding points in layers differing in azimuthal orientation are not unique. In particular, the centers of the empty octahedra are displaced in turn by [1/3, −1/3] and [1/3, 1/3]. As a result, a two-layer repeat distance in the first case displaces the origin by [−2/3, 0] and in the second by [2/3, 0], so there was not sufficient justification for choosing a nonminimal obtuse β.

Reversal of the b axis gives the form $\{100/0\bar{1}0/\bar{1}0\bar{1}\}$ to the matrix for forward and inverse transformation of the coordinate axes in the two systems, and the coordinates transform in accordance with the matrix $\{10\bar{1}/0\bar{1}0/00\bar{1}\}$. After the coordinate systems had been referred to a common origin (the shift in the origins is characterized by the vector [0.390; 0.250; 0.224]), the atomic coordinates were deduced from the x-ray data for direct comparison with the electron-diffraction

TABLE 3. Rotation Angles of Tetrahedron and Octahedron Base Edges in Projection on ab

| O in tetrahedron bases		O, OH in octahedron bases		OH in octahedron bases	
edge	α	edge	α	edge	α
Si_1 tetrahedron		Al_1 octahedron			
$O_1 - O_2$	4°50'	$O_5 - OH_1$	6°10'	$OH_2 - OH_3$	8°15'
$O_1 - O_3$	2°30'	$O_4 - OH_1$	9°10'	$OH_2 - OH_4$	6°30'
$O_2 - O_3$	2°30'	$O_4 - O_5$	6°10'	$OH_3 - OH_4$	5°35'
Mean	3°17'	Mean	7°10'	Mean	6°47'
Si_2 tetrahedron		Al_2 Octahedron			
$O_1 - O_2$	4°45'	$O_5 - OH_1$	4°45'	$OH_2 - OH_3$	7°10'
$O_1 - O_3$	2°30'	$O_4 - OH_1$	8°30'	$OH_2 - OH_4$	4°10'
$O_2 - O_3$	2°30'	$O_4 - O_5$	7°20'	$OH_3 - OH_4$	5°40'
Mean	3°15'	Mean	6°52'	Mean	5°40'
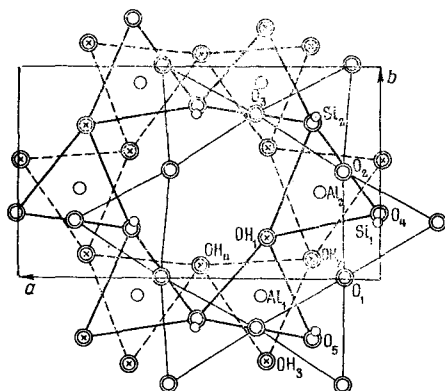
Fig. 2. A σ_1 layer of nacrite in normal projection on the ab plane. The heavy solid lines are the tops of octahedra, while the dashed lines are their bases and the thin lines are the bases of tetrahedra.
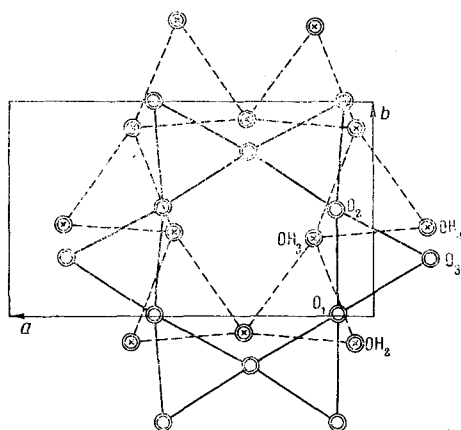

Fig. 3. Mutual disposition of the O atoms in tetrahedron bases and OH in octahedron faces in adjacent layers. See Fig. 2 for symbols.

data (Table 1). We used the numbering of [5] for convenience in this comparison. Figures 2 and 3 show the positions and numbering of the atoms.

Table 1 shows that the two sets of results in general agree well, e.g., the planes containing the Al and Si atoms almost coincide, and there is agreement over the deviations of the O atoms and OH groups from a single plane for the contacting outter surfaces of adjacent layers. On the other hand, there are certain marked differences between the two sets of results, e.g., the z coordinates of the O atoms in tetrahedron bases and of OH groups in octahedron faces. The electron-diffraction results make the tetrahedron bases and the octahedron OH groups more remote from the Si and Al respectively. The elongation of the tetrahedra is well seen from the length difference between the basal and side edges (Table 2). The interatomic distances of Table 2 on average agree with the corresponding values in [5]; the differences are confined to particular points, with electron diffraction giving somewhat longer side edges of the octahedra and shorter bonds between layers. The mean interatomic distances for each polyhedron have the relations found for regular polyhedra, which confirms the conclusions of [11].

The most pronounced differences are between the angles of ditrigonal rotation for the bases of the tetrahedra and octahedra. The structural polyhedra are unequally distorted, so it is difficult to state any single rotation angles. We calculated the angles between particular base edges in the initial and refined structures in projection on the ab plane. Table 3 shows that these angles for the tetrahedron bases are substantially less than those in the other kaolin minerals kaolinite and dickite [2, 10] (7.5-10°) and than those for nacrite as found by x-ray methods (about 7.3°) [5]. On the other hand, the OH in octahedron bases have larger angles (relative to the trigonal initial pattern), but they remain somewhat less than those for O and OH in octahedron bases.

This result is completely supported by general arguments on the effects of ditrigonal rotation in layer silicates composed of two-level layers [5]. The displacement directions for O atoms in tetrahedron bases in kaolinite and dickite are governed by attraction from the octahedral cations in their own layer and from the hydrogen bonds to OH groups in the adjacent layer, which act in the same sense on account of the cubic packing of the layer anions. The octahedral cations in the adjacent layer on normal projection onto ab fall at the centers of tetrahedron bases and in this respect have no effect on the latter. In nacrite, the cations within a layer have the same role, as do the hydrogen bonds, but the cations in the adjacent layer act in the opposite sense because of the hexagonal anion packing in the layer. This factor appears unable to overcome or balance out the joint effect of the other two factors, but it reduces appreciably the ditrigonal rotation angle of the tetrahedra. This effect is not reflected in the x-ray results [5].

Octahedron base rotation is accompanied by edge shortening for given a and b. The above displacement of the bases from the central cations is required to maintain acceptable distances from the cations to the oxygen vertices.

A good characterization of the layer distortion and mutual disposition is provided by the actual relative displacements of the grids of tetrahedra and octahedra that are revealed by the refinement. The atomic coordinates (Table 1) show that the relative displacements of the centers of the Al and Si hexagons are characterized by the following displacements in the ab system of nacrite: $\sigma_1(0.345;$ $0.345)$, $\sigma_2(0.345; -0.345)$, $\tau_3(0.005; -0.315)$, $\tau_6(0.005;$ $0.315)$. The real values of σ and τ give detail to the causes of the above deviation from the ideal β, and they show to what extent this arises from uniform shear deformation of the layers $(\Delta\sigma_x = 0.012)$ and from additional interlayer displacements $(\Delta\tau_x = 0.005)$. The result is that, over a repeat distance, the origin in projection on ab is displaced by $2(\sigma_x$

$+ \tau_x)a = 0.700a$, which is equivalent to a displacement of $-0.300\ a$.

One consequence of these deviations of the displacements from ideal ones (multiples of $a/3$, b) is that we no longer have collinear vectors for the interlayer displacements as reckoned between the centers of Si hexagons; in projection on ab they form a zigzag sequence of the combinations $\tau_6 + \sigma_2$, $\tau_3 + \sigma_1 - [0.350; -0.030]$, $[0.350; 0.030]$, so we no longer can accept the arguments presented [5] to justify the choice of the larger $\beta > \pi/2$.

This study has shown that high-voltage electron diffraction is highly effective in structure analysis of minerals and that it should be used whether or not x-ray studies have been made.

LITERATURE CITED

1. S. B. Hendricks, Z. Kristall., 85, 345 (1939).
2. R. E. Newnham, Min. Mag., 32, 683 (1961).
3. B. B. Zvyagin and A. D. Shcheglov, Dokl. Akad. Nauk SSSR, 142, No. 1 (1962).
4. B. B. Zvyagin, Kristallografiya, 7, 51 (1962) [Sov. Phys.—Crystallogr., 7, 38 (1962)].
5. A. M. Blount, I. M. Threadgold, and S. W. Bailey, Clays and Clay Minerals, 17, 3 (1969).
6. B. B. Zvyagin, Electron Diffraction and Structural Crystallography of Clay Minerals [in Russian], Nauka, Moscow (1964).
7. B. B. Zvyagin, A. F. Fedotov, S. V. Soboleva, and K. S. Mishchenko, Kristallografiya, 17, No. 4 (1972) (in press).
8. S. V. Soboleva and B. B. Zvyagin, Kristallografiya, 13, 605 (1968) [Sov. Phys.—Crystallogr., 13, 516 (1969)].
9. B. K. Vainshtein, Structural Electron Diffraction [in Russian], Izd. AN SSSR, Moscow (1956).
10. B. B. Zvyagin, Kristallografiya, 5, 40 (1960) [Sov. Phys.—Crystallogr., 5, 32 (1960)].
11. V. A. Drits, Kristallografiya, 15, 913 (1970) [Sov. Phys.—Crystallogr., 15, 795 (1971)].